



Synthesis, stereoelectronic characterization and antiparasitic activity of new 1-benzenesulfonyl-2-methyl-1,2,3,4-tetrahydroquinolines

Romina J. Pagliero^a, Sabrina Lusvardi^{a,†}, Adriana B. Pierini^b, Reto Brun^c, María R. Mazzieri^{a,*}

^aDepartamento de Farmacia, Facultad de Ciencias Químicas, Universidad Nacional de Córdoba, Córdoba, Argentina

^bDepartamento de Química Orgánica, INFIQ, Facultad de Ciencias Químicas, Universidad Nacional de Córdoba, Córdoba, Argentina

^cParasite Chemotherapy, Swiss Tropical Institute, CH-4002 Basel, Switzerland

ARTICLE INFO

Article history:

Received 28 August 2009

Revised 4 November 2009

Accepted 5 November 2009

Available online 10 November 2009

Keywords:

Antiparasitic

Benzenesulfonyl

Tetrahydroquinolines

Stereoelectronic properties

ABSTRACT

The synthesis and full 3D structural characterization of nine new 1-benzenesulfonyl-2-methyl-1,2,3,4-tetrahydroquinoline derivatives are reported. These belong to a library whose rationale for the design was the previous knowledge of the biological relevant properties of both structural moieties. From protozoan antiparasitic screening, compounds **3** demonstrated interesting activity against *Trypanozoma cruzi* with low cytotoxicity. Besides, most compounds were moderately active against *Plasmodium falciparum*. Of these, **3** and **9** can be considered as lead scaffolds for further optimization. The substituent on BS did not influence the 3D structure properties and the ¹H NMR spectra revealed the existence of an intramolecular weak hydrogen bond, C–H...O=S. Molecular modeling and X-ray crystallography also confirmed this finding, which is relevant to compound conformational preference.

© 2009 Elsevier Ltd. All rights reserved.

1. Introduction

Approximately two million people are estimated to die each year from parasitic diseases such as malaria, african (sleeping sickness) and american trypanosomiasis (Chagas disease) and leishmaniasis.¹ Furthermore, these parasitic infections are frequently associated with immunocompromised patients and are thus also seen in developed countries. Malaria is the most prevalent and pernicious protozoan parasitic disease in humans. According to the last WHO report,² half of the world's population is at risk from malaria which is caused by Plasmodium parasites. Four species of Plasmodium commonly infect humans, but two of them in particular, *Plasmodium falciparum* (*P. falciparum*) and *Plasmodium vivax*, account for the majority of cases of morbidity and mortality. The effective artemisinin-based combination therapies have resulted in success in more than 90% of cases. However, WHO announced recently that the emergence of artemisinin resistant parasites could seriously undermine the global malaria control efforts thus far achieved.^{2,3} Sleeping sickness is caused by the parasites *Trypanosoma brucei rhodesiense* (*T.b. rhodesiense*) and *Trypanosoma brucei gambiense*. Only four drugs are registered for the treatment of human african trypanosomiasis and all of them have a certain level of toxicity. However, treatment is mandatory because the disease

is fatal if left untreated. In South America, a different Trypanosome causes Chagas disease, *Trypanosoma cruzi* (*T. cruzi*). This parasite is transmitted by bloodsucking reduviid bugs.⁴ The infection is an important cause of mortality and morbidity and no vaccines or safe and effective chemotherapeutic agents are available. A similar situation account for leishmaniasis, caused by the protozoan parasite *Leishmania*.⁵ So, there is an urgent need for new, safe and effective drugs against these parasitic infections, since many of those currently in use have major problems.⁶ Furthermore, there is a considerable evidence that extended use of these drugs is leading to the development of resistance.

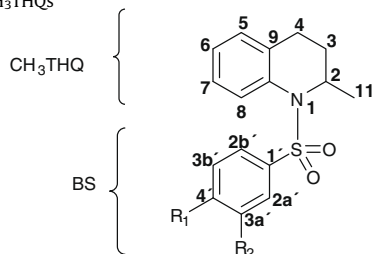
As part of an ongoing lead discovery project and on the basis of our experience in the field,^{7,8} we are interested in the synthesis and screening of series of *N*-benzenesulfonyl derivatives of bioactive heterocyclic compounds. One of this series is 1-benzenesulfonyl-2-methyl-1,2,3,4-tetrahydroquinoline (BS-CH₃THQ) **1–10**, which is depicted in Table 1. These new BS-CH₃THQs incorporate two key structural and biological units in their molecules: a benzenesulfonyl (BS) and a 2-methyl-1,2,3,4-tetrahydroquinoline (CH₃THQ). Indeed, CH₃THQ has shown interesting and diverse pharmacological activities such as antibacterial,⁹ antioxidant,⁹ NMDA antagonist,¹⁰ antiplatelet aggregation¹¹ and antiarrhythmic,¹² among others. On the other hand, BS is a substituent frequently present in molecules with biological activity. Not only is the *p*-aminobenzenesulfonyl moiety a known PABA antagonist with antibacterial and antileprotic activity, but the BS group bound to different heterocycles has led to analogs displaying similar or better biological activities than their precursors.^{13–21} Therefore, the combination of a BS and a biologically active heterocycle, such as CH₃THQ, appears to be a very promising

* Corresponding author. Tel./fax: +54 351 4334163.

E-mail addresses: mrmazzie@fcq.unc.edu.ar, maria_mazzieri@yahoo.com.ar (M.R. Mazzieri).

[†] Present address: Chemistry Department, Carnegie Mellon University, 4400 5th Ave, Pittsburgh, PA, USA.

Table 1
Synthesised BS-CH₃THQs



Compd	R ₁ ^a	R ₂	Yield ^b	Mp ^c (lit.)	%Purity ^d
1	H	H	82	104–104.5	98.28
2	NHCOCH ₃	H	54	195–196	98.25
3	NO ₂	H	78	159–160	97.83
4	CH ₃	H	81	79–80 (84–85) ^e	97.15
5	F	H	68	121–121.5	95.73
6	Cl	H	67	92–92.5	96.53
7	Br	H	65	80–80.5	96.41
8	OCH ₃	H	66	91–92	96.62
9	H	NO ₂	70	115–115.5	98.37
10	NH ₂	H	79	154–155	98.45

^a Structures were proved by analytical HRMS and by ¹H and ¹³C NMR. (¹H, ¹³C, COSY, HSQC, HMBC) spectrometry and FT-IR spectroscopy.

^b Isolated yields.

^c Uncorrected.

^d Measure by HPLC.

^e See Refs. 22,23.

hypothesis for drug discovery. With this in mind a major screening for different activities is presently being carried out for the compounds.

Our research has been focused on exploring the consequences of a BS linkage through a *N* on the stereoelectronic properties of the heterocycle for CADD applications, using either ligand-based or structure-based molecular design methods. When a BS moiety is bound to heterocycles through nitrogen, it has two ways of modulating its stereoelectronic properties and ultimately the biological activity. It could intramolecularly influence the heterocyclic ring or interact with the target through intermolecular forces.^{8,24} Bearing this in mind, we synthesized ten BS-CH₃THQ compounds, of which nine are new. These ten compounds had different substituent at the phenyl moiety (R₁/R₂, Table 1). The selection of them was mainly guided by electronic considerations as defined by Hammett constant, σ .²⁵ In this way, different groups (from electron-donating, such as NH₂ ($\sigma = -0.66$) to electron-withdrawing, such as NO₂ ($\sigma = 0.78$)) were included.

In the present work we report the synthesis, 2D and 3D structural characterization and in vitro activity against protozoan parasites of novel BS-CH₃THQ.

2. Results and discussion

2.1. Chemistry

Scheme 1 outlines the synthetic strategy for compounds **1–10**. The preparation of CH₃THQ was carried out by reduction of quinoxaline heterocycle as previously reported.²⁶ The synthesis of **1–9** was accomplished in one step with good yields (54–82% of isolated products), by condensation of CH₃THQ with the appropriate and commercially available benzenesulfonyl chloride, under nitrogen atmosphere. The reaction was carried out in pyridine as basic media. The sulfonylation time was around 1 h, except for **2** (3 h). The reaction was stopped by addition of HCl 10%, which facilitated the isolation of the product as a colored solid. Compound **10** was achieved in two steps procedure (Scheme 1). First, the *N*-acetyl-sulfonyl-CH₃THQ (**2**) was prepared, which was subsequently

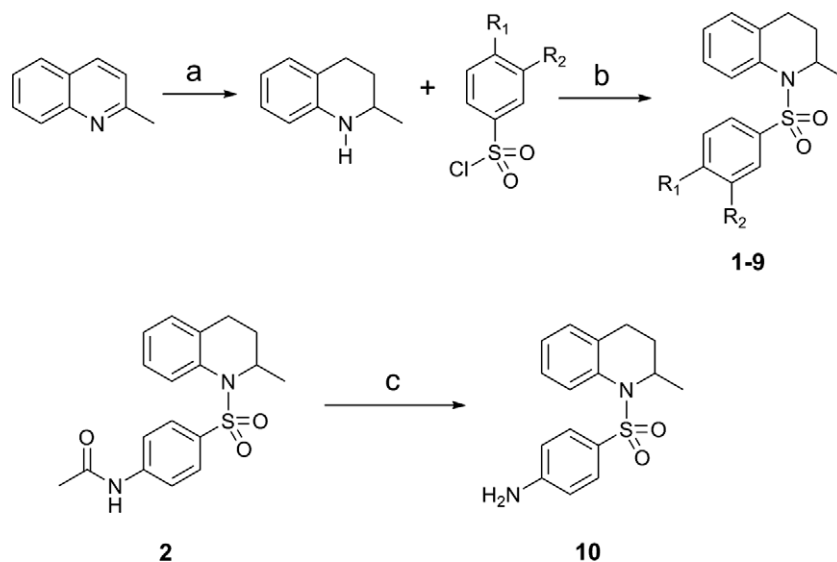
hydrolyzed with HCl 4 M in acetone, affording the *p*-amine derivative (**10**) after 3 h. Crystalline and stable compounds were obtained after work-up and purification processes as described in the experimental section. All products were obtained with purity higher than 96%.

In the literature have been described many synthesis methods for the incorporation of BS group in the anular *N*, most of them include the cyclization step to obtain BS-heterocycles and also tedious work-ups.^{22,23,27–30} The criteria followed for the selection of the present method was based on its simplicity and good yield. The procedure has also provided a facile access to derivatives of 1-benzenesulfonyl benzotriazol.⁷ Furthermore, the library could be enlarged including other nitrogenated-heterocycles and different substitutions at BS since many benzenesulfonyl chlorides are currently commercially available. On the other hand, the simplicity of the work-up and purification procedures would make possible to apply this method to automation system for parallel synthesis.

NMR, FT-IR and HRMS were used to provide complete structural characterization of **1–10**. An extensive NMR analysis was performed for both the structural characterization and future Quantitative Structure Stereoelectronic Relationship studies. The ¹H NMR spectrum (DMSO-*d*₆) of **1–10** showed signals at δ lower than 5 ppm that accounted for the five aliphatic protons of the CH₃THQ ring, plus those of the CH₃. The protons of the CH₃ group on BS of **2**, **4** and **8** were also in that region. All the aromatic protons appeared at δ values higher than 7 ppm. Furthermore, the ¹³C NMR spectrum of **1–10** showed the aliphatic carbons appearing between 22–55 ppm, and aromatic carbons between 112 and 170 ppm along with C=O signals of **2**. The complete and unambiguous ¹H and ¹³C NMR assignments were achieved using a combination of COSY, HSQC and HMBC experiments (see Supplementary data for spectra).

The NMR spectra of **3** will be used here as example to explain the assignment of signals to the structure (δ are in ppm and *J* in Hz, refer to Table 1 for atom numbering). The doublet of quartets at δ _H 4.41 was assigned to H2, which directly correlated to C2 (δ _C 53.03) and H11 (δ _H 1.20). The chemical shift of H2 was consistent with the proximity of N1, with the multiplicity being due to the coupling with CH₃ (δ _H 1.20, d, *J*_{H11–H2} 6.5) and both enantiotopic H3 (*J*_{H2–H3a} 6.8; *J*_{H2–H3b} 6.4). The two signals corresponding to both of the H3 appeared at δ _H 1.30/1.85 (¹*J* –13.3) and correlated with C3 (δ _C 30.23). The same was observed with signals of the two enantiotopic H4 at 1.72/2.42 (¹*J* –15.8) which correlated with the two H3 (*J*_{H3a–H4a} 8.5; *J*_{H3b–H4a} 5.2; *J*_{H3a–H4b} 5.3; *J*_{H3b–H4b} 6.8) and with C4 (δ _C 24.46). The signal at δ _H 7.09 (dd, *J*_{H5–H6} 7.3 and *J*_{H5–H7} 1.0) was assigned to H5, and was confirmed by HMBC experiments (³*J* correlation with C4, δ _C 24.46) and by COSY experiments with ²*J* with H6 (δ _H 7.16, td, *J*_{H6–H5} 7.3; *J*_{H6–H7} 7.7 and *J*_{H6–H8} 0.8). The H7 signal appeared at δ _H 7.27 (td, *J*_{H7–H6} 7.7; *J*_{H7–H8} 7.8 and *J*_{H7–H5} 1.0), and finally the H8 at 7.56 (dd, *J*_{H8–H7} 7.8 and *J*_{H8–H6} 0.8). Also, the ³*J* correlations between H5, H6, H7 and H8 were also clearly observed in COSY and were therefore consistent with the assignment described. Furthermore, the analysis was supported by HMBC ³*J* correlations between H5–C7, H6–C8, H7–C5 and H8–C6, thus allowing us to assign C6 (δ _C 126.50), C7 (δ _C 127.24), C8 (δ _C 126.85) and C5 (δ _C 128.91). The two remaining signals in the proton aromatic area corresponded to the BS group; H2' appeared at δ _H 7.74 and H3' at δ _H 8.31. Both signals showed the expected variation in chemical shifts due to the substitution in the *para* position of the BS.

On the other hand, four nonprotonated carbon signals observed in ¹³C NMR were assigned as follows: 134.04 (C9), 134.37 (C10), 144.19 (C1') and 150.41 (C4'). The key correlations found in HMBC led us to an unambiguous assignment of these carbons. Compounds **1**, **2**, **4–10** showed similar NMR spectra, with the assignments been made under the same considerations described above for **3** (see spectra in Supplementary data).



Scheme 1. Synthesis of BS-CH₃THQ. Reagents and conditions: (a) NaBH₄/NiCl₂·6H₂O, methanol, 25 °C; (b) anhydrous pyridine, 25 °C; (c) HCl 4 M, acetone, 90 °C.

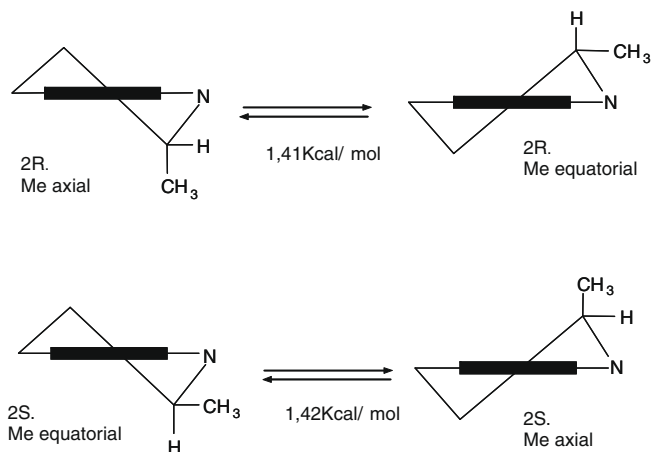


Figure 1. Four theoretical half-chair conformations of CH₃THQ. Difference of energy between the CH₃ in the ax or eq position for each enantiomer is shown under the arrows.

2.2. Computational modeling

Conformational studies of **1–10** were performed with the semiempirical (AM1) and DFT (B3LYP/6-31G(d)) methods as implemented in GAUSSIAN 03.³¹ First of all, the preferred conformation of CH₃THQ was studied at the B3LYP/6-31G(d) level of theory. CH₃THQ could present either a half-chair or a half-boat conformation for each enantiomer (2R or 2S). Figure 1 shows the possible half-chair conformers viewed down an imaginary axis toward the heterocycle, with the CH₃ group axial (ax) or equatorial (eq). The theoretical analysis showed a maximum difference of 1.4 kcal/mol between CH_{3ax} and CH_{3eq}, with the expected preferences for the methyl group in the equatorial position (91.76%). On the other hand, the four half-boat possible conformations were not stable. In agreement, Charifson et al.¹⁸ were unable to find a stable boat conformation for tetrahydroisoquinolines.

Once the minimum-energy conformation was found for the heterocycle, the BS moiety was added, and the whole molecule (BS-CH₃THQ) was minimized using AM1 semiempirical method. The conformational search was carried out for both enantiomers (2R or 2S) through a careful systematic scan of relevant dihedral angles

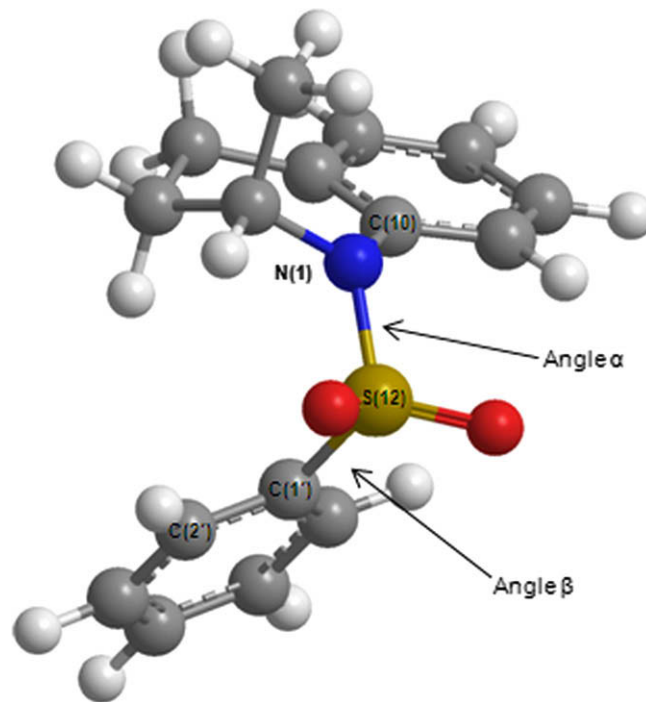


Figure 2. Minimum structure of **1** obtained by B3LYP/6-31G(d). Angles α and β were scanned in the conformational search of BS-CH₃THQs.

in order to inspect the positioning of sulfonyl (α angle) and phenyl (β angle) substituents (Fig. 2). A full geometry optimization at the B3LYP/6-31G(d) level of theory was later performed for the lowest energy conformations found. Finally, each minimum was characterized as a stationary point by vibrational frequency calculations. For all the derivatives the number of imaginary frequencies was zero.

The BS group was shown to be pseudo-axial for all energy-minimized conformations. No significant difference in energy or relevant geometric parameters (α and β angles) were found between the 2R and 2S enantiomers (data not shown). Each enantiomer of BS-CH₃THQs has four minimum-energy conformations,

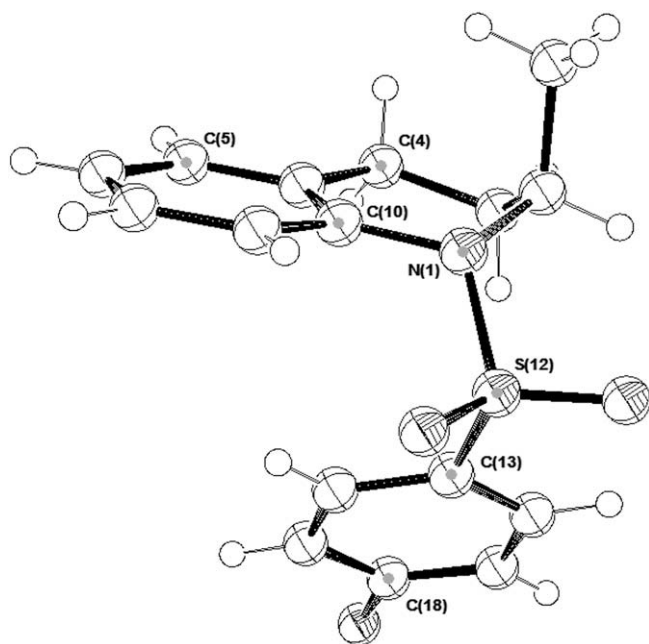


Figure 3. ORTEP representation of the R enantiomer of 5.

two with $\text{CH}_{3\text{ax}}$ and two with $\text{CH}_{3\text{eq}}$. For the conformers with $\text{CH}_{3\text{eq}}$ the torsion angle α displayed the minimum between $293\text{--}297^\circ$ and between $135\text{--}137^\circ$. For α values of $293\text{--}297^\circ$, β showed a minimum at $76\text{--}78^\circ$; and for α $135\text{--}137^\circ$, β was $137\text{--}140^\circ$. A similar situation was found for the conformers with $\text{CH}_{3\text{ax}}$. The torsion angle α showed a minimum between $293\text{--}295^\circ$ and between $78\text{--}96^\circ$. For α $293\text{--}295^\circ$, the torsion angle β had a minimum at $79\text{--}81^\circ$; for α $78\text{--}96^\circ$, β was $61\text{--}69^\circ$. The values found for these relevant angles were independent of the substituent in BS moiety (see Supplementary data). On the other hand, for both enantiomers, the conformers with the $\text{CH}_{3\text{ax}}$ were 5 kcal/mol (99.9%) more stable than those with $\text{CH}_{3\text{eq}}$, showing a higher difference of energy between both conformers ($\text{CH}_{3\text{eq}}$ and $\text{CH}_{3\text{ax}}$) than unsubstituted CH_3THQ (1.4 kcal/mol, Fig. 1). The ΔE informed in both cases is Zero Point Corrected. Including the solvent (DMSO) through Tomasi's continuum polarized model did not modify this energy difference.

The NMR spectral data and theoretical conformational analysis were in agreement with the presence of the half-chair conformation with the $\text{CH}_{3\text{ax}}$ for **1–10**. For NMR data, at room temperature, each set of methylene protons on the piperidine ring of CH_3THQ (for 3- CH_2 and 4- CH_2) exhibited an AB pattern. Four distinct signals were observed for the geminal protons $\text{H}_{3\text{a}}/\text{H}_{3\text{b}}$ and $\text{H}_{4\text{a}}/\text{H}_{4\text{b}}$, indicating that no conformational average was taking place. The four signals were well resolved and the multiplicities were in agreement with pseudo-axial and pseudo-equatorial positions ($^2J_{\text{gem}} = 13.3$ and 15.8 for $\text{H}_{3\text{a}}/\text{H}_{3\text{b}}$ and $\text{H}_{4\text{a}}/\text{H}_{4\text{b}}$ respectively; $^3J_{\text{ax;ax}} = \text{ce:hsp sp} = 0.25^\circ > 8.6$, $^3J_{\text{ax;eq}} = 5.4$ and $^3J_{\text{eq;eq}} = 6.4$). The problem of the dynamic geminal proton interchange in six member non-saturated heterocyclic rings has been extensively described by Katrietzky et al.³² Chilmonczyk et al.³³ and Amm et al.³⁴ Moreover, the presence of two equivalent coupling constant between the $\text{H}_2\text{--H}_{3\text{a}}$ and $\text{H}_2\text{--H}_{3\text{b}}$ is fully explained if the methyl group is in an axial position so that the H_2 roughly bisects the two protons H_3 . The 'V' conformation of the molecule, given by the presence of the BS group in the pseudo-axial position, makes the Me_{ax} position preferred over the Me_{eq} .

Further confirmation of the orientation of $\text{CH}_{3\text{ax}}$ was made by the X-ray crystallography analysis of the compounds (Fig. 3). Table

Table 2
Comparison of structures obtained by theoretical calculation and X-ray

Parameter	Theoretical calcd value	X-ray value
Torsion angle α	65.31°	64.92°
Torsion angle β	99.19°	105.99°
Angle $\text{C}_{10}\text{--N}_1\text{--S}$	119.34°	116.88°
Angle $\text{N}_1\text{--S--C}_1^{\text{a}}$	107.66°	107.74°
Distance $\text{C}_6\text{--C}_4^{\text{b}}$	6.29 \AA	6.84 \AA
Distance $\text{C}_4\text{--C}_4^{\text{b}}$	5.68 \AA	5.12 \AA
Distance $\text{H}_8\text{--O}$	2.27 \AA	2.44 \AA
Angle $\text{C}_8\text{--H}_8\text{--O}$	115.3°	109°

^a Calculated with GAUSSIAN 03 at level of theory B3LYP 6-31G*.

^b In ORTEP representation $\text{C}_{18} = \text{C}_4'$ and $\text{C}_{13} = \text{C}_1'$.

2 describes some significant parameters of the geometry obtained by theoretical calculations and X-ray crystallography.[‡]

Another interesting observation was the presence of the signal of H_8 at a higher chemical shift (around δ 7.59) than the same proton of unsubstituted CH_3THQ (δ 6.42), which implied a 1.17 ppm average downfield. Also, the H_8 appeared at a lower field than the remaining H of the spin system. The same behavior was found when NMR spectra were calculated by using a B3LYP/6-31G(d) level of theory. This unexpected unshielding of H_8 may have been caused by a dipolar interaction (hydrogen bond) with one oxygen of the BS group. Sanchez-Viesca et al. demonstrated evidence of $\text{C--H}\cdots\text{O}$, $\text{C--H}\cdots\text{N}$ and $\text{C--H}\cdots\text{Cl}$ hydrogen bonds in thiazole,³⁵ benzopyridine³⁶ and propionitriles³⁷ derivatives by ^1H NMR experiments with the presence of two intramolecular weak H-bonds of the type $\text{C--H}\cdots\text{O}$ in the benzopyridine derivatives leading to a $\Delta\delta$ of 1.0–1.2 ppm.³⁶ Furthermore, based on crystallographic data, Desiraju et al.^{38,39} observed distances of 2.0–3.0 Å between $\text{H}\cdots\text{O}$, when the H-bond $\text{C--H}\cdots\text{O}$ occurred in crystals, for more than 100 analyzed structures. For BS- CH_3THQ , **1–10**, the calculated geometry showed a distance of 2.28–2.39 Å between $\text{H}\cdots\text{O}$ in all minimum conformations, thus supporting the possibility of an intramolecular H-bond between $\text{C}_8\text{--H}\cdots\text{O}$. Another parameter used by Desiraju^{38,39} and Taylor⁴⁰ to describe the H-bond of the type $\text{C--H}\cdots\text{O}$ is the angle between these three atoms. They observed by X-ray experiment that $\text{C--H}\cdots\text{O}$ angles between $90\text{--}130^\circ$ corresponded to the formation of weak H-bonds. This was true in the case of BS- CH_3THQ s which showed values of between $109\text{--}123^\circ$. However, it should be mentioned that the opposite effect was reported by Charifson et al.¹⁸ for the H_8 of benzyltetrahydroquinoline, which showed a lower chemical shift than expected. In this case, the dramatic upfield shift was explained as a consequence of the position of H_8 within the shielding cone of the adjacent phenyl group. From the conformational geometry shown by **1–10** it can be appreciated that H_8 is clearly distant from the shielding cone of the phenyl of BS moiety. The SO_2 linkage conferred the typical butterfly-like conformation to the compounds,^{41,42} which was clearly different than the one from CH_2 linkage.

2.3. Antiprotozoal activity

Compounds **1–10** were tested against *T. b. rhodesiense*, *T. cruzi*, *Leishmania donovani*, and *P. falciparum* as well as for cytotoxicity against rat skeletal myoblasts (L-6). All the activity determinations were carried out at the Screening Center of the Swiss Tropical Institute. These results are presented in Table 3.

As a general observation, all compounds exhibited low cellular toxicity (at least more than 590-fold lower) compared to pod-

[‡] CCDC 744103 contains the supplementary crystallographic data for this paper. These data can be obtained free of charge from The Cambridge Crystallographic Data Centre via http://www.ccdc.cam.ac.uk/data_request/cif.

Table 3
Antiparasitic activity of compounds **1–10** expressed as IC₅₀ (μM)^a

	<i>T. b. rhodesiense</i> IC ₅₀	<i>T. cruzi</i> IC ₅₀	<i>L. donovani</i> IC ₅₀	<i>P. falciparum</i> . K1 ^b IC ₅₀	Cytotoxicity. L-6 IC ₅₀	SI <i>T. cruzi</i> ^c	SI <i>P. falciparum</i> ^c
Melarsoprol	0.008						
Benznidazole		1.54					
Miltefosine			0.25				
Chloroquine				0.25			
Podophyllotoxin					0.01		
CH ₃ THQ	87.25	188.73	>611.33	>33.96	248.61	1.32	7.32
1	52.86	21.26	174.12	13.25	70.03	3.29	5.28
2	49.79	21.45	50.68	>14.53	52.02	2.42	3.58
3	153.14	11.44	>271.02	8.31	248.28	21.70	30.00
4	43.99	16.61	22.52	11.03	4.90	0.29	0.44
5	124.62	223.74	167.07	12.10	67.57	0.30	5.58
6	43.50	15.98	18.87	8.43	20.46	1.28	2.43
7	40.09	13.78	21.35	6.65	7.36	0.53	1.10
8	43.85	15.89	26.74	11.79	5.99	0.37	0.5
9	33.06	31.94	24.93	10.34	186.97	5.85	18.08
10	37.20	19.73	55.81	>16.55	35.27	1.78	2.13

^a Values represent the average of four determinations (two determinations of two independent experiments); errors for individual measurements differed by less than 50%.

^b Resistant to chloroquine and pyrimethamine.

^c Selectivity Index calculated as SI = IC₅₀L6/IC₅₀ parasite.

phyllotoxin which was used as a reference. The antiparasitic potential of all compounds was analyzed by applying the WHO/TDR screening activity criteria specified for each parasite.⁶ Four compounds (**3**, **6**, **7** and **9**) showed moderate growth inhibition of *P. falciparum* with IC₅₀ values around or below 10 μM. Moreover, two of these compounds (**3** and **9**) had a good selectivity index (30.0 and 18.1, respectively). In line with the WHO/TDR activity criteria, all compounds with the exception of **5** were moderately active against *T. cruzi*. Compound **3** was the most active, with an IC₅₀ of 11.4 μM, which implies only a sevenfold reduced potency when compared to that of benznidazole as the reference (IC₅₀ 2.13 μM). Due to the interesting antiplasmodial activity and the low cytotoxicity (IC₅₀ of 248 μM), compound **3** represents a promising lead scaffold for further structural optimization. Compounds **7** and **8** showed moderate growth inhibition toward *L. donovani* (18.9 and 21.3 μM). Among the newly prepared derivatives, none of them presented activity against *T. b. rhodesiense* (IC₅₀ >50 μM).

2.4. Structure–activity relationships

In general, the presence of BS moiety decreased IC₅₀ with respect to the heterocycle precursor, the only exceptions being the compounds **3** and **5** against *T. b. rhodesiense* and **5** against *T. cruzi*. On the other hand, the presence of different substituents on the BS seemed to have a particular influence depending on the parasite. Only the *p*-fluoro substitution (**5**) showed a general negative impact on the antiparasitic activity.

Overall, the lowest IC₅₀ values and highest potencies of the series were towards *T. cruzi*. The *para* substitution on the BS resulted in an increase of activity with the only exception being **2** which had almost the same activity as **1**. The substitution with a strong electron-withdrawing group such as nitro in *para* (**3**) resulted in the most active compound of this series. On the other hand, *meta*-substitution on the BS seemed to be unfavorable for the in vitro activity against *T. cruzi*. Indeed a change of the nitro from *para* (**3**) to *meta* (**9**) reduced the activity threefold and resulted in one of the least active analogue. For *L. donovani* activity, two halogenated compounds (**7** and **8**) showed moderate growth inhibition. Even though the potency was low when compared to miltefosine, the addition of the BS substituent strongly increased the potency by about 35-fold, with respect to the CH₃THQ. The same effect was observed against *P. falciparum* but less pronounced, with the addition of the BS increasing the activity by threefold at best. The potency of compounds **1–10** against *P. falciparum* was challenging, and also some REA analysis could be

performed. The addition of an electron-withdrawing substituent was clearly favorable and led to the most potent analogues (**3**, **6**, **7** and **9**) while electron-donating (**10**) decreased the activity. In the light of our results on molecular modeling, the substituent on BS did not influence the 3D structure properties of **1–10**. Besides, no linear correlation could be found with any single variable such as electronic, lipophilic or steric parameters (data not shown). So, a combination of the electronic distribution on the phenyl group, the size of the substituent and the lipophilicity of the compounds could explain the differences on the antiparasitic activity.

3. Conclusions

We have reported on the design, synthesis and antiparasitic activity of a small library of *N*-substituted benzenesulfonyl derivatives of CH₃THQ. The cytotoxicity on rat skeletal myoblast (L-6) was evaluated as well. Also, a complete characterization and theoretical conformational analysis were carried out. Detailed NMR investigation including ¹H and ¹³C NMR, HSQC, HMBC data, were consistent with structures of compounds **1–10**. From spectra and molecular modeling data we were able to conclude that the 'V' conformation of the molecules, given by the presence of the BS moiety bound to the CH₃THQ affected the stereoelectronic properties of the heterocycle, thus making the Me_{ax} position preferred over the Me_{eq}. However, the *para* or *meta* substituents on BS did not influence the 3D structure properties of the heterocycle or the molecules as a whole. On the other hand, computational and NMR data were in agreement with the presence of just one chair conformation with the CH_{3ax}, and also with the occurrence of an H-bond between C8–H and one of the oxygen of SO₂.

The series was tested against four parasites, with moderate activities being found. The new derivatives **1–10** demonstrated to be selective among the four protozoan parasites. *T. cruzi* and *P. falciparum* appeared to be the most sensitive of them. In spite of the small number of compounds in the series, some interesting inhibitors against *T. cruzi* and *P. falciparum* were discovered. Compounds **3** and **9** showed moderate growth inhibition of *P. falciparum* with IC₅₀ values below 10 μM and good cytotoxicity. We identified these two compounds as being lead-candidates for antiplasmodial activity.⁴³ On the other hand, compound **3** also presented interesting activity against *T. cruzi* with only fivefold reduced potency compared to benznidazole as the reference drug. Due to this moderate antitrypanosomal activity and the low cytotoxicity (IC₅₀ = 248 μM), compound **3** represents a promising lead scaffold for

further structural optimization. These findings suggest that productive criteria were used in the design strategy. Further investigations into these BS-CH₃THQs structures are ongoing based on three strategies: (1) enlarging the present series using parallel synthetic tools, (2) QSAR studies using multiparametric regression analysis and (3) application of CADD to identify the target proteins and the mode of action.

4. Experimental

4.1. General considerations

Melting points (mp) were determined using an electrothermal apparatus, by microcapillary methods and are uncorrected. Infrared spectra were recorded on a Nicolet 5 SXC FT-IR. NMR experiments were performed on a Bruker advance II 400 Hz, ultra shield TM spectrometer at 400.16(¹H) and 100.62(¹³C) which has an inverse multinuclear detection sonda, digital resolution and a variable temperature unite. Chemical shift values are reported in ppm (δ) and were taken with DMSO-*d*₆ as a solvent (referred to residual DMSO at 2.50 ppm for ¹H and 39.5 ppm for ¹³C). Coupling constants (*J*) are in Hz (refer to Table 1 for atom numbering). The multiplicities of the signals are described using the following abbreviations s = singlet, d = doublet, t = triplet, q = quartet, sex = sextet, m = multiplet. High resolution mass spectroscopy experiments were taken in a Micromass Q-TOF micro Hybrid Quadrupole/Orthogonal High Resolution Time of Flight MS with Micromass capillary HPLC (Waters Corporation).

All the benzenesulfonyl chlorides were purchased from Sigma-Aldrich. The pyridine used for the synthesis was previously distilled and stored over pellets of NaOH. The 2-methyl-1,2,3,4-tetrahydroquinoline (CH₃THQ) was prepared by catalytic hydrogenation of 2-methyl-quinoline (Aldrich + 95%) as described by Atsuko et al.²⁶ Reaction progress was monitored by TLC (Silica Gel 60 F₂₅₄, Merck) visualizing with UV light. The silica gel used in the purification of the products was Merck grade 60, 230–400 mesh, 60A. All others reagents and solvents were used as purchased from Anhedra.

4.2. Experimental procedure, spectral data for compounds 1–10

4.2.1. General procedures for the synthesis

Compounds 1–9 were synthesized by adding 4.00 mmol of an appropriate substituted benzenesulfonyl chloride to a solution of CH₃THQ (3.00 mmol, 0.44 g, 0.43 mL) in 1.5 mL of anhydrous pyridine at room temperature. The reaction mixture was vigorously stirred at 60–80° until no more starting materials could be detected by TLC (hexane/acetone 7:3). This mixture was then cooled at –5 °C and chilled water was added to precipitate the product. The solid was filtered off, washed exhaustively with HCl 0.01 M and water, and dried over CaCl₂ and anhydrous MgSO₄. Colored solids were obtained at yields of 70–85%.

Compound 10 was synthesized by hydrolysis of compound 2: 3 mmol (1.03 g) of 2 were dissolved in 18 mL of acetone, heated at 40 °C and 10 mL HCl 4 M was added dropwise. After that, the reaction mixture was heated at 60–70° and stirred for 3 h, until no more starting material could be detected by TLC (hexane/acetone 5:5). The mixture was cooled and a solution of NaCO₃ was added to pH 9. The acetone was evaporated in vacuum and the solid filtered off, before being washed with water and dried over CaCl₂ and anhydrous MgSO₄. A white solid was obtained at a yield of 92%.

4.2.2. General procedure for purification of the derivatives

The products isolated as described previously were then purified as follows: (A) All the compounds were obtained as a colored

solid from the reaction mixture. To eliminate the colored impurities, the compounds were dissolved in hexane/acetone 7:3 and filtered through a mixture of Silica Gel 60 and active carbon. The solvent was evaporated in vacuum and was dried over CaCl₂ for 24 h. A light yellow solid resulted with a yield of 92–98%. (B) Some derivatives seemed to discompose in silica gel. These were washed with cold ethanol (–5 °C) to eliminate the colored impurities. The yields were 84–86% of a pink solid. (C) All compounds were finally recrystallized from ethanol or methanol to give 78–88% of the products as white or yellow crystals.

4.2.3. Specific procedures and spectral data for compounds 1–10

4.2.3.1. 1-(Benzenesulfonyl)-2-methyl-1,2,3,4-tetrahydroquinoline (1). (R₁ = H; R₂ = H). Purification by procedures A and C (ethanol). White crystals (0.71 g, 82%) mp 104.0–104.5 °C (from EtOH). IR ($\nu_{\max}/\text{cm}^{-1}$, KBr): 3065 (CH_{aromatic}), 2927 (CH_{3 asim}), 1343 (SO_{2 asim}), 1168 (SO_{2 sim}). ¹H NMR (DMSO-*d*₆, 400.16 Hz): 7.63 (tt, 1H, 7.2 and 1.2 Hz, H4'); 7.59 (d, 1H, 8.0 Hz, H8); 7.54 (d, 2H, 8.0 Hz, H2'); 7.50 (dt, 2H, 7.4 and 1.2 Hz, H3'); 7.3 (td, 1H, 7.8 and 1.2 Hz, H7); 7.10 (td, 1H, 7.4 and 1.1 Hz, H6); 7.08 (d, 1H, 6.8 Hz, H5); 4.3 (sex, 1H, 6.6 Hz, H2); 2.4 (m, 1H, H4b); 1.8 (m, 1H, H3b); 1.7 (m, 1H, H4a); 1.3 (m, 1H, H3a); 1.2 (d, 3H, 6.4 Hz, H11). ¹³C NMR (DMSO-*d*₆, 100.62 Hz; assigned using HSQC): 139.4 (Cq-1'); 135.6 (Cq-10); 134.4 (Cq-9); 134.2 (Cq-4'); 130.3 (CH-3'); 129.3 (CH-5); 127.6 (CH-8); 127.6 (CH-2'); 127.5 (CH-7); 126.7 (CH-6); 53.0 (CH-2); 30.5 (CH₂-3); 24.9 (CH₂-4); 22.5 (CH₃-11). COSY: ²J_{gem}: H3a–H3b, H4a–H4b. ³J_{vec}: H2–H3a; H2–H3b; H2–H11; H3a–H4a; H3a–H4b; H3b–H4b; H3b–H4a. ³J_{ortho}: H6–H7; H5–H6; H7–H8; H2'–H3'; H3'–H4'. ⁴J_{meta}: H5–H7; H6–H8; H2'–H4'. HMBC (DMSO-*d*₆, *f*₁ = 400.16 Hz, *f*₂ = 100.62 Hz) (C→H): C11→H2, H3b; C4→H5, H3a, H3b; C3→H2, H4a, H4b, H11; C2→H4a, H4b, H3a, H3b, H11; C6→H8; C7→H5; C8→H6; C2'→H4'; C5→H7, H4a, H4b; C4'→H2'; C9→H8, H6, H4a, H4b, H3a, H3b; C10→H7, H5, H2, H4a, H4b; C1'→H3'. HRMS (EI) calcd mass for C₁₆H₁₇NO₂S: 287.0980; found: 287.0988.

4.2.3.2. 1-(4-Acetamide-benzenesulfonyl)-2-methyl-1,2,3,4-tetrahydroquinoline (2). (R₁ = NHCOCH₃; R₂ = H). Purification by procedures A and C (ethanol). White crystals (0.56 g, 54%) mp 195.0–196.5 °C (from EtOH). IR ($\nu_{\max}/\text{cm}^{-1}$, KBr): 3352 (NH), 3066 (CH_{aromatic}), 2932 (CH_{3 asim}), 2858 (CH_{3 sim}), 1703 (CO), 1334 (SO_{2 asim}), 1310 (CN_{amida}), 1157 (SO_{2 sim}). ¹H NMR (DMSO-*d*₆, 400.16 Hz): 10.3 (s, 1H, H5'); 7.9 (d, 1H, 7.9 Hz, H8); 7.6 (d, 2H, 9.2 Hz, H3'); 7.4 (d, 2H, 8.8 Hz, H2'); 7.2 (td, 1H, 7.6 and 1.5 Hz, H7); 7.1 (td, 1H, 7.4 and 1.6 Hz, H6); 7.0 (dd, 1H, 7.2 and 0.8 Hz, H5); 4.3 (sex, 1H, 6.6 Hz, H2); 2.4 (m, 1H, H4b); 2.0 (s, 3H, H7'); 1.8 (m, 1H, H3b); 1.7 (m, 1H, H4a); 1.3 (m, 1H, H3a); 1.2 (d, 3H, 6.8 Hz, H11). ¹³C NMR (DMSO-*d*₆, 100.62 Hz; assigned using HSQC): 170.2 (C6'=O); 144.4 (Cq-4'); 135.7 (Cq-10); 134.3 (Cq-9); 133.0 (Cq-1'); 129.2 (CH-5); 128.9 (CH-2'); 127.5 (CH-8); 127.5 (CH-7); 126.5 (CH-6); 119.5 (CH-3'); 52.8 (CH-2); 30.5 (CH₂-3); 25.1 (CH₃-7'); 24.9 (CH₂-4); 22.5 (CH₃-11). COSY: ²J_{gem}: H3a–H3b, H4a–H4b. ³J_{vec}: H2–H3a; H2–H3b; H2–H11; H3a–H4a; H3a–H4b; H3b–H4b; H3b–H4a. ³J_{ortho}: H6–H7; H5–H6; H7–H8; H2'–H3'. ⁴J_{meta}: H5–H7; H6–H8. HMBC (DMSO-*d*₆, *f*₁ = 400.16 Hz, *f*₂ = 100.62 Hz) (C→H): C11→H2; C4→H5, H3a, H3b; C3→H2, H4a, H4b, H11; C2→H4b, H3a, H3b, H11; C3'→H5', H2'; C6→H8; C7→H5; C8→H6; C5→H7, H4b; C1'→H3', H2'; C9→H8, H6, H4a, H4b, H3a, H3b; C10→H7, H5, H2, H4a, H4b; C4'→H2', H3', H5'; C6'→H5', H7'. HRMS (EI) calcd mass for C₁₈H₂₀N₂O₃S: 344.1194; found: 344.1208.

4.2.3.3. 1-(4-Nitro-benzenesulfonyl)-2-methyl-1,2,3,4-tetrahydroquinoline (3). (R₁ = NO₂; R₂ = H). Purification by procedures A and C (ethanol). Yellow crystals (0.83 g, 78%) mp 159.0–160.0 °C (from EtOH). IR ($\nu_{\max}/\text{cm}^{-1}$, KBr): 3111 (CH_{aromatic}), 2970, 2932

(CH₃), 1527 (NO₂ asim), 1347 (SO₂ asim), 1308 (NO₂ sim), 1166 (SO₂ sim). ¹H NMR (DMSO-*d*₆, 400.16 Hz): 8.3 (d, 2H, 9.4 Hz, H3'); 7.7 (d, 2H, 8.8 Hz, H2'); 7.6 (d, 1H, 7.6 Hz, H8); 7.3 (td, 1H, 8.4 and 1.2 Hz, H7); 7.2 (td, 1H, 7.4 and 0.8 Hz, H6); 7.0 (d, 1H, 7.2 Hz, H5); 4.4 (sex, 1H, 6.6 Hz, H2); 2.4 (m, 1H, H4b); 1.8 (m, 1H, H3b); 1.7 (m, 1H, H4a); 1.3 (m, 1H, H3a); 1.2 (d, 3H, 5.8 Hz, H11). ¹³C NMR (DMSO-*d*₆, 100.62 Hz; assigned using HSQC): 150.4 (Cq-4'); 144.2 (Cq-1'); 134.4 (Cq-10); 134.0 (Cq-9); 128.9 (CH-5); 128.7 (CH-2'); 127.2 (CH-7); 126.8 (CH-8); 126.6 (CH-6); 125.1 (CH-3'); 53.0 (CH-2); 30.2 (CH₂-3); 25.5 (CH₂-4); 19.6 (CH₃-11). COSY: ²J_{gem}: H3a-H3b, H4a-H4b. ³J_{vec}: H2-H3a; H2-H3b; H2-H11; H3a-H4a; H3a-H4b; H3b-H4b; H3b-H4a. ³J_{ortho}: H6-H7; H5-H6; H7-H8; H2'-H3'. ⁴J_{meta}: H5-H7; H6-H8. HMBC (DMSO-*d*₆, *f*₁ = 400.16 Hz, *f*₂ = 100.62 Hz) (C→H): C11→H2; C4→H5, H3a, H3b; C3→H2, H4a, H4b, H11; C2→H4b, H4a, H3b, H11; C3'→H2'; C6→H8; C8→H6, H7; C7→H5; C5→H7, H4b; C9→H8, H6, H4a, H4b, H3a, H3b; C10→H7, H5, H2, H4a, H4b; C1'→H3', H2'; C4'→H2', H3'. HRMS (EI) calcd mass for C₁₂H₁₆N₂O₄S: 355.0728; found: 355.0729.

4.2.3.4. 1-(4-Methyl-benzenesulfonyl)-2-methyl-1,2,3,4-tetrahydroquinoline (4). (R₁ = CH₃; R₂ = H). Purification by procedures A and C (methanol). White crystals (073 g, 81%) mp 79–80 °C (from MeOH). IR (ν_{max}/cm⁻¹, KBr): 3066 (CH_{aromatic}), 2949, 2858 (νCH₃), 1341 (SO₂ asim), 1159 (SO₂ sim). ¹H NMR (DMSO-*d*₆, 400.16 Hz): 7.5 (d, 1H, 8.0 Hz, H8); 7.34 (d, 2H, 8.4 Hz, H2'); 7.29 (d, 2H, 8.0 Hz, H3'); 7.2 (td, 1H, 7.4 and 1.2 Hz, H7); 7.1 (td, 1H, 7.6 and 1.2 Hz, H6); 7.0 (dd, 1H, 8.0 and 0.8 Hz, H5); 4.3 (sex, 1H, 6.5 Hz, H2); 2.4 (m, 1H, H4b); 2.3 (s, 3H, H5'); 1.8 (m, 1H, H4a); 1.7 (m, 1H, H3b); 1.3 (m, 1H, H3a); 1.2 (d, 3H, 6.4 Hz, H11). ¹³C NMR (DMSO-*d*₆, 100.62 Hz; assigned using HSQC): 144.6 (Cq-4'); 136.8 (Cq-1'); 135.7 (Cq-10); 134.2 (Cq-9); 130.7 (CH-3'); 129.3 (CH-5); 127.7 (CH-2'); 127.5 (CH-7); 127.4 (CH-8); 126.6 (CH-6); 52.9 (CH-2); 30.4 (CH₂-3); 24.9 (CH₂-4); 22.4 (CH₃-11); 22.0 (CH₃-5'). COSY: ²J_{gem}: H3a-H3b, H4a-H4b. ³J_{vec}: H2-H3a; H2-H3b; H2-H11; H3a-H4a; H3a-H4b; H3b-H4b; H3b-H4a. ³J_{ortho}: H6-H7; H5-H6; H7-H8; H2'-H3'. ⁴J_{meta}: H5-H7; H6-H8. HMBC (DMSO-*d*₆, *f*₁ = 400.16 Hz, *f*₂ = 100.62 Hz) (C→H): C5'→H3'; C11→H2, H3a, H3b; C4→H5, H3a, H3b; C3→H2, H4a, H4b, H11; C2→H4b, H3a, H11; C6→H8, H5; C8→H6; C7→H5; C5→H7, H4b, H4a; C3'→H5'; C9→H8, H6, H4a, H4b, H3a, H3b; C10→H7, H5, H2, H4a, H4b; C1'→H3', H2'; C4'→H2', H3'. HRMS (EI) calcd mass for C₁₇H₁₉NO₂S: 301.1136; found: 301.1135.

4.2.3.5. 1-(4-Fluoro-benzenesulfonyl)-2-methyl-1,2,3,4-tetrahydroquinoline (5). (R₁ = F; R₂ = H). Purification by procedures B and C (ethanol). White crystals (0.67 g, 68%) mp 121.0–121.5 °C (from EtOH). IR (ν_{max}/cm⁻¹, KBr): 3076 (CH_{aromatic}), 2973, 2858 (CH₃), 1343 (SO₂ asim), 1171 (SO₂ sim); 1008 (CF). ¹H NMR (DMSO-*d*₆, 400.16 Hz): 7.59 (d, 1H, 7.6 Hz, H8); 7.56 (qt, 2H, 8.8 and 2.0 Hz, J_{HF(meta)} = 5.2 Hz, H2'); 7.4 (tt, 2H, 8.8 and 2.4 Hz, J_{HF(ortho)} = 9.2 Hz, H3'); 7.3 (td, 1H, 7.6 and 1.2 Hz, H7); 7.2 (td, 1H, 7.4 and 1.2 Hz, H6); 7.1 (d, 1H, 7.6 Hz, H5); 4.4 (sex, 1H, 5.6 Hz, H2); 2.4 (m, 1H, H4b); 1.8 (m, 1H, H3b), 1.7 (m, 1H, H4a); 1.3 (m, 1H, H3a); 1.2 (d, 3H, 6.4 Hz, H11). ¹³C NMR (DMSO-*d*₆, 100.62 Hz; assigned using HSQC): 165.0, ¹J_{HF} = 240.6 Hz (Cq-4'); 135.3, ⁴J_{CF} = 2.89 Hz (Cq-1'); 134.9 (Cq-10); 133.9 (Cq-9); 130.2, ³J_{CF} = 9.51 Hz (CH-2'); 128.8 (CH-5); 127.0 (CH-7); 127.0 (CH-8); 126.2 (CH-6); 116.9, ²J_{CF} = 22.6 Hz (CH-3'); 52.6 (CH-2); 30.0 (CH₂-3); 24.4 (CH₂-4); 22.0 (CH₃-11). COSY: ²J_{gem}: H3a-H3b, H4a-H4b. ³J_{vec}: H2-H3a; H2-H3b; H2-H11; H3a-H4a; H3a-H4b; H3b-H4b; H3b-H4a. ³J_{ortho}: H6-H7; H5-H6; H7-H8; H2'-H3'. ⁴J_{meta}: H5-H7; H6-H8. HMBC (DMSO-*d*₆, *f*₁ = 400.16 Hz, *f*₂ = 100.62 Hz) (C→H): C11→H2, H3a, H3b; C4→H5, H3a, H3b; C3→H2, H4a, H4b, H11; C2→H4a, H4b, H3a, H3b, H11; C3'→H2'; C6→H8, H7; C8→H6, H7; C7→H5; C5→H7, H4b, H4a; C9→H8, H6, H4a, H4b, H3a, H3b; C10→H7, H5, H2, H4a, H4b; C1'→H3'; C4'→H2', H3'.

HRMS (EI) calcd mass for C₁₆H₁₆FNO₂S: 328.0783; found: 328.0781.

4.2.3.6. 1-(4-Chloro-benzenesulfonyl)-2-methyl-1,2,3,4-tetrahydroquinoline (6). (R₁ = Cl; R₂ = H). Purification by procedures B and C (ethanol). White crystals (0.69 g, 67%) mp 92.0–92.5 °C (from EtOH). IR (ν_{max}/cm⁻¹, KBr): 3071 (CH_{aromatic}), 2965, 2860 (νCH₃), 1344 (SO₂ asim), 1169 (SO₂ sim); 758 (CCl). ¹H NMR (DMSO-*d*₆, 400.16 Hz): 7.62 (dd, 2H, 8.80 and 2.20 Hz, H2'); 7.58 (d, 1H, 8.0 Hz, H8); 7.5 (dd, 2H, 8.8 and 2.2 Hz, H3'); 7.3 (td, 1H, 7.6 and 1.6 Hz, H7); 7.2 (td, 1H, 7.6 and 1.2 Hz, H6); 7.1 (d, 1H, 7.20 Hz, H5); 4.4 (sex, 1H, 6.5 Hz, H2); 2.5 (m, 1H, H4b); 1.9 (m, 1H, H3b), 1.7 (m, 1H, H4a); 1.3 (m, 1H, H3a); 1.2 (d, 3H, 6.8 Hz, H11). ¹³C NMR (DMSO-*d*₆, 100.62 Hz; assigned using HSQC): 139.1 (Cq-1'); 138.3 (Cq-4'); 135.3 (Cq-10); 134.5 (Cq-9); 130.4 (CH-2'); 129.6 (CH-3'); 129.3 (CH-5); 127.6 (CH-7); 127.4 (CH-8); 126.8 (CH-6); 53.2 (CH-2); 30.6 (CH₂-3); 25.0 (CH₂-4); 22.5 (CH₃-11). COSY: ²J_{gem}: H3a-H3b, H4a-H4b. ³J_{vec}: H2-H3a; H2-H3b; H2-H11; H3a-H4a; H3a-H4b; H3b-H4b; H3b-H4a. ³J_{ortho}: H6-H7; H5-H6; H7-H8; H2'-H3'. ⁴J_{meta}: H5-H7; H6-H8. HMBC (DMSO-*d*₆, *f*₁ = 400.16 Hz, *f*₂ = 100.62 Hz) (C→H): C11→H2, H3b; C4→H5, H3a, H3b; C3→H2, H4a, H4b, H11; C2→H4a, H4b, H3a, H3b, H11; C6→H8, H5; C8→H6, H7; C7→H5; C5→H7, H4b, H4a; C3'→H2'; C9→H8, H6, H4a, H4b, H3a, H3b; C10→H7, H5, H2, H4a, H4b, H3a, H3b; C4'→H2', H3'; C1'→H3', H2'. HRMS (EI) calcd mass for C₁₆H₁₆ClNO₂S: 344.0488; found: 344.0505.

4.2.3.7. 1-(4-Bromo-benzenesulfonyl)-2-methyl-1,2,3,4-tetrahydroquinoline (7). (R₁ = Br; R₂ = H). Purification by procedures B and C (ethanol). White crystals (0.76 g, 65%) mp 80.0–80.5 °C (from EtOH). IR (ν_{max}/cm⁻¹, KBr): 3068 (CH_{aromatic}), 2973, 2916 (CH₃), 1344 (SO₂ asim), 1168 (SO₂ sim); 605 (CBr). ¹H NMR (DMSO-*d*₆, 400.16 Hz): 7.8 (d, 2H, 8.4 Hz, H3'); 7.6 (d, 1H, 8.4 Hz, H8); 7.5 (d, 2H, 8.4 Hz, H2'); 7.3 (td, 1H, 7.8 and 1.0 Hz, H7); 7.2 (td, 1H, 7.4 and 0.8 Hz, H6); 7.1 (dd, 1H, 7.2 and 0.8 Hz, H5); 4.4 (sex, 1H, 6.56 Hz, H2); 2.5 (m, 1H, H4b); 1.9 (m, 1H, H3b), 1.7 (m, 1H, H4a); 1.3 (m, 1H, H3a); 1.2 (d, 3H, 6.8 Hz, H11). ¹³C NMR (DMSO-*d*₆, 100.62 Hz; assigned using HSQC): 138.7 (Cq-1'); 135.3 (Cq-10); 134.5 (Cq-9); 133.4 (CH-3'); 129.6 (CH-2'); 129.4 (CH-5); 128.2 (Cq-4'); 127.7 (CH-7); 127.5 (CH-8); 126.9 (CH-6); 53.3 (CH-2); 30.7 (CH₂-3); 25.0 (CH₂-4); 22.6 (CH₃-11). COSY: ²J_{gem}: H3a-H3b, H4a-H4b. ³J_{vec}: H2-H3a; H2-H3b; H2-H11; H3a-H4a; H3a-H4b; H3b-H4b; H3b-H4a. ³J_{ortho}: H6-H7; H5-H6; H7-H8; H2'-H3'. ⁴J_{meta}: H5-H7; H6-H8. HMBC (DMSO-*d*₆, *f*₁ = 400.16 Hz, *f*₂ = 100.62 Hz) (C→H): C11→H2, H3a, H3b; C4→H5, H3a, H3b; C3→H2, H4a, H4b, H11; C2→H4a, H4b, H3a, H3b, H11; C6→H8, H7; C8→H6; C7→H5; C4'→H2', H3'; C5→H7, H4a, H4b; C9→H8, H6, H5, H4a, H4b, H3a, H3b; C10→H7, H5, H8, H2, H4a, H4b, H3a, H3b; C1'→H3', H2'. HRMS (EI) calcd mass for C₁₆H₁₆BrNO₂S: 387.9983; found: 387.9979.

4.2.3.8. 1-(4-Methoxy-benzenesulfonyl)-2-methyl-1,2,3,4-tetrahydroquinoline (8). (R₁ = OCH₃; R₂ = H). Purification by procedures A and C (ethanol). White crystals (0.67 g, 66%) mp 91.0–92.0 °C (from EtOH). IR (ν_{max}/cm⁻¹, KBr): 3066 (CH_{aromatic}), 2970, 2932 (CH₃), 2840 (OCH₃ asim), 1338 (SO₂ asim), 1158 (SO₂ sim). ¹H NMR (DMSO-*d*₆, 400.16 Hz): 7.5 (dd, 1H, 8.4 and 0.8 Hz, H8); 7.4 (dd, 2H, 8.8 and 2.0 Hz, H2'); 7.2 (td, 1H, 8.0 and 1.5 Hz, H7); 7.1 (td, 1H, 7.6 and 1.47 Hz, H6); 7.05 (dd, 1H, 7.2 and 1.2 Hz, H5); 7.01 (dd, 2H, 8.8 and 2.0 Hz, H3'); 4.3 (sex, 1H, 6.4 Hz, H2); 3.8 (s, 1H, H6'); 2.4 (m, 1H, H4b); 1.8 (m, 1H, H3b); 1.7 (m, 1H, H4a); 1.3 (m, 1H, H3a); 1.2 (d, 3H, 6.4 Hz, H11). ¹³C NMR (DMSO-*d*₆, 100.62 Hz; assigned using HSQC): 163.7 (Cq-4'); 135.8 (Cq-10); 134.2 (Cq-9); 131.3 (Cq-1'); 129.9 (CH-2'); 129.3 (CH-5); 127.5 (CH-7); 127.5 (CH-8); 126.5 (CH-6); 115.4 (CH-3'); 56.7 (CH₃-5'); 52.8 (CH-2); 30.4 (CH₂-3); 24.9 (CH₂-4); 22.4 (CH₃-11).

COSY: $^2J_{gem}$: H3a–H3b, H4a–H4b. $^3J_{vec}$: H2–H3a; H2–H3b; H2–H11; H3a–H4a; H3a–H4b; H3b–H4b; H3b–H4a. $^3J_{ortho}$: H6–H7; H5–H6; H7–H8; H2'–H3'. $^4J_{meta}$: H5–H7; H6–H8. HMBC (DMSO- d_6 , $f_1 = 400.16$ Hz, $f_2 = 100.62$ Hz) (C→H): C11→H2; C4→H5, H3a, H3b; C3→H2, H4a, H4b, H11; C2→H4a, H4b, H11; C6→H8; C8→H6; C7→H5; C5→H7, H4b; C1'→H3'; C9→H8, H6, H5, H4a, H4b, H3a; C10→H7, H5, H8, H2, H4a, H4b; C4'→H2', H3'. HRMS (EI) calcd mass for $C_{17}H_{19}NO_3S$: 340.0983; found: 340.0979.

4.2.3.9. 1-(3-Nitro-benzenesulfonyl)-2-methyl-1,2,3,4-tetrahydroquinoline (9). (R₁ = H; R₂ = NO₂). Purification by procedures A and C (ethanol). White crystals (0.52 g, 70%) mp 115.0–115.5 °C (from EtOH). IR (ν_{max}/cm^{-1} , KBr): 3111 (CH_{aromatic}), 2970, 2932 (CH₃), 1531 (NO₂ asim), 1352 (SO₂ asim), 1352 (NO₂ sim), 1170 (SO₂ sim). 1H NMR (DMSO- d_6 , 400.16 Hz): 8.5 (ddd, 1H, 8.0, 2.4 and 1.2 Hz, H4'); 8.1 (t, 1H, 2.0 Hz, H2'a); 7.85 (dt, 1H, 8.0 and 1.2 Hz, H2'b); 7.81 (t, 1H, 7.81 Hz, H3'b); 7.6 (dd, 1H, 8.4 and 1.0 Hz, H8); 7.3 (dd, 1H, 7.8 and 1.3 Hz, H7); 7.2 (td, 1H, 7.4 and 1.2 Hz, H6); 7.1 (dd, 1H, 7.2 and 0.8 Hz, H5); 4.4 (sex, 1H, 6.8 Hz, H2); 2.4 (m, 1H, H4b); 1.8 (m, 1H, H3b); 1.6 (m, 1H, H4a); 1.3 (m, 1H, H3a); 1.2 (d, 3H, 6.4 Hz, H11). ^{13}C NMR (DMSO- d_6 , 100.62 Hz; assigned using HSQC): 148.1 (Cq-3'a); 140.0 (Cq-1'); 134.5 (Cq-10 and Cq-9); 132.9 (C2'b); 131.9 (C3'b); 128.9 (CH-5); 128.3 (C4'); 127.4 (CH-7); 127.1 (CH-8); 126.7 (CH-6); 121.8 (CH-2'a); 51.9 (CH-2); 30.6 (CH₂-3); 24.7 (CH₂-4); 22.3 (CH₃-11). COSY: $^2J_{gem}$: H3a–H3b, H4a–H4b. $^3J_{vec}$: H2–H3a; H2–H3b; H2–H11; H3a–H4a; H3a–H4b; H3b–H4b; H3b–H4a. $^3J_{ortho}$: H6–H7; H5–H6; H7–H8; H3'b–H2'b; H3'b–H4'. $^4J_{meta}$: H5–H7; H6–H8; H2'b–H2a; H2'b–H4'; H2'a–H4'. HMBC (DMSO- d_6 , $f_1 = 400.16$ Hz, $f_2 = 100.62$ Hz) (C→H): C11→H2; C4→H5, H3a, H3b; C3→H2, H4a, H4b, H11; C2'→H4a, H4b, H11; C2'a→H4', H2'b; C6H8; C8→H6; C7→H5; C4'→H2'a, H2'b, H3'b; C5→H7; C3'b→H4'; C2'b→H4', H2'a, H3'b; C9→H8, H6, H4a, H4b, H3a, H3b; C10→H7, H5, H2, H4a, H4b; C1'→H2'a, H3'b; C3'a→H2'a, H3'b. HRMS (EI) calcd mass for $C_{16}H_{16}N_2O_4S$: 355.0728; found: 355.0724.

4.2.3.10. 1-(4-Amino-benzenesulfonyl)-2-methyl-1,2,3,4-tetrahydroquinoline (10). (R₁ = NH₂; R₂ = H). Purification by procedure C (methanol). Beige crystals (0.71 g, 79%) mp 154.0–155.0 °C (from EtOH). IR (ν_{max}/cm^{-1} , KBr): 3469, 3373 (NH), 3252 (CH_{aromatic}), 2933, 2858 (ν_{CH_3}), 1640 (NH), 1319 (SO₂ asim), 1154 (SO₂ sim). 1H NMR (DMSO- d_6 , 400.16 Hz): 7.6 (d, 1H, 8.4 Hz, H8); 7.2 (td, 1H, 7.8 and 1.6 Hz, H7); 7.11 (td, 1H, 6.4 and 0.8 Hz, H6); 7.10 (d, 2H, 7.6 Hz, H2'); 7.06 (dd, 1H, 7.6 and 1.6 Hz, H5); 6.5 (d, 2H, 8.4 Hz, H3'); 6.0 (s, 1H, H5'); 4.3 (sex, 2H, 6.5 Hz, H2); 2.4 (m, 1H, H4b); 1.9 (m, 1H, H4a); 1.8 (m, 1H, H3b); 1.3 (m, 1H, H3a); 1.2 (d, 3H, 6.8 Hz, H11). ^{13}C NMR (DMSO- d_6 , 100.62 Hz; assigned using HSQC): 154.0 (Cq-4'); 136.3 (Cq-10); 134.0 (Cq-9); 129.6 (CH-2'); 129.2 (CH-5); 127.6 (CH-8); 126.1 (CH-6); 124.5 (Cq-1'); 124.2 (CH-7); 113.6 (CH-3'); 52.3 (CH-2); 30.1 (CH₂-3); 25.0 (CH₂-4); 22.3 (CH₃-11). COSY: $^2J_{gem}$: H3a–H3b, H4a–H4b. $^3J_{vec}$: H2–H3a; H2–H3b; H2–H11; H3a–H4a; H3a–H4b; H3b–H4b; H3b–H4a. $^3J_{ortho}$: H6–H7; H5–H6; H7–H8; H2'–H3'. $^4J_{meta}$: H5–H7; H6–H8. J with NH2: H3'–H5'; H2'–H5'. HMBC (DMSO- d_6 , $f_1 = 400.16$ Hz, $f_2 = 100.62$ Hz) (C→H): C11→H2, H3a, H3b; C4→H5, H3a, H3b; C3→H2, H4a, H4b, H11; C2→H4b, H4a, H3a, H3b, H11; C3'→H5'; C1'→H3', H2'; C6→H8; C7→H5; C8→H6; C5→H7, H4b, H4a; C2'→H3', H5'; C9→H8, H6, H7, H4a, H4b, H3a, H3b; C10→H7, H5, H8, H6, H2, H4a, H4b; C4'→H2'. HRMS (EI) calcd mass for $C_{16}H_{18}N_2O_2S$: 302.1089; found: 302.1073.

4.2.4. Purity of compounds 1–10

All compounds were tested for purity by High Performance Liquid Chromatography (HPLC). The HPLC system consisted of an Agilent 1000 series solvent delivery system coupled with an auto-

mated injector system and a UV–visible detector. The column used was a Water RP-C18 (50 × 3 mm) with particles of 3 μ m which was maintained at room temperature. A flow rate of 1.0 mL/min with methanol–water 70:30 mixtures was used as mobile phase. Detection was made at 254 nm and the injection volume was 20 μ L. The inspection of the chromatograms showed a purity of more than 96% for all the compounds (see Table 1), measured as the percentage of area under the sample peak. The solvent peak (methanol) was observed at 0.578.

The melting point ranges were also measured as criteria of purity, and are reported with the spectral data in the previous section.

4.2.5. Computational data of compounds 1–10

All the BS-CH₃THQ derivatives were first minimized with the semiempirical AM1 method. The conformational search was carried out for both enantiomers (2R or 2S) through a careful systematic scan of the relevant dihedral angles (α and β angles) using the 'Opt = ModRedundant' keyword in GAUSSIAN 03³¹ with 36 steps of 10° each. The preference of the 2-CH₃ group for the axial or equatorial position was also studied for both enantiomers. The potential energy surface was explored to find the global minima by scanning the C10–N1–S12–C1' torsion angle (α angle). Then, for each minimum thus found, the N1–S12–C1'–C2' torsion angle (β angle) was scanned at fixed α . A full geometry optimization[§] at the B3LYP/6-31G(d) level of theory was later performed for the lowest energy conformations found. Finally, each minimum was characterized as a stationary point by vibrational frequency calculations ('freq = noraman'). For all the derivatives the number of imaginary frequencies was zero. Molecular orbitals, Mulliken charges, and the charges fitting to the electrostatic potential were calculated. The NMR spectrum were also calculated using a B3LYP/6-31G(d) level of theory as well as for HF/6-31G(d). In both cases the 'nmr = giao' method was used for the NMR calculation with no specification of the symmetry ('nosym').

4.2.6. Antiprotozoal activity

The in vitro activities against the protozoan parasites *T.b. rhodesiense*, *T. cruzi*, *L. donovani* and *P. falciparum* as well as cytotoxicity were determined as described earlier.⁴⁴ Compounds were measured in duplicate in the range of 0.2–300 μ M. The following substances were used as reference standards: melarsoprol (*T.b. rhodesiense*), benznidazole (*T. cruzi*), miltefosine (*L. donovani*), chloroquine (*P. falciparum*) and podophyllotoxin (cytotoxicity assay using L-6 cells).

Acknowledgments

This work was supported by SECyT-UNC (Argentina). R.J.P. and S.L. acknowledge CONICET fellowships. Dr. Paolo Carvalho for HRMS and X-ray. Bonetto Gloria for NMR techniques assistance.

Supplementary data

Supplementary data associated with this article can be found, in the online version, at doi:10.1016/j.bmc.2009.11.010.

References and notes

- WHO. World health report 2004 statistical annex; <http://www.who.int/whr/2004/annex/en/index.html>.
- WHO. World Malaria Report 2008; <http://apps.who.int/malaria/wmr2008/>.
- WHO. Drug Resistance Could Set Back Malaria Successes http://new.paho.org/hq/index.php?option=com_content&task=view&id=769&Itemid=259.

[§] Command line for gaussian03: B3LYP/6-31G(d) opt(loose)nosym scf(maxcycles = 500) pop = full iop(6/7 = 3) pop = mk gfpint.

4. WHO. Chagas disease; http://www.who.int/topics/chagas_disease/en/.
5. WHO. Leishmaniasis; <http://www.who.int/topics/leishmaniasis/en/>.
6. Nwaka, S.; Hudson, A. *Nat. Rev. Drug Disc.* **2006**, *5*, 941.
7. Hergert, L. Y.; Nieto, M. J.; Becerra, M. C.; Albesa, I.; Mazzieri, M. R. *Lett. Drug Des. Disc.* **2008**, *5*, 313.
8. Nieto, M. J.; Alovero, F. L.; Manzo, R. H.; Mazzieri, M. R. *Eur. J. Med. Chem.* **2005**, *40*, 361.
9. Johnson, J. V.; Rauchman, B. S.; Baccanari, D. P.; Roth, B. J. *Med. Chem.* **1989**, *32*, 1942.
10. Leeson, P. D.; Carling, R. W.; Moore, K. W.; Moseley, A. M.; Smith, J. D.; Stevenson, G.; Chan, T.; Baker, R.; Foster, A. C.; Grimwood, S., et al. *J. Med. Chem.* **1992**, *35*, 1954.
11. Yang, J.; Hua, W. Y.; Wang, F. X.; Wang, Z. Y.; Wang, X. *Bioorg. Med. Chem.* **2004**, *12*, 6547.
12. Kimura, T.; Imanishi, S.; Arita, M. J. *Cardiovasc. Pharmacol.* **1989**, *13*, 767.
13. Davis, M. C.; Franzblau, S. G.; Martin, A. R. *Bioorg. Med. Chem. Lett.* **1998**, *8*, 843.
14. Lee, S.; Oh, S.; Park, G. M.; Kim, T. S.; Ryu, J. S.; Choi, H. K. *Korean J. Parasitol.* **2005**, *43*, 123.
15. Pinheiro, T. R.; Yunes, R. A.; Lopez, S. N.; Santecchia, C. B.; Zacchino, S. A.; Cechinel Filho, V. *Arzneimittelforschung* **1999**, *49*, 1039.
16. Garuti, L.; Roberti, M.; Cermelli, C. *Bioorg. Med. Chem. Lett.* **1999**, *9*, 2525.
17. Garuti, L.; Roberti, M.; Rossi, T.; Cermelli, C.; Portolani, M.; Malagoli, M.; Castelli, M. *Anticancer Drug Des.* **1998**, *13*, 397.
18. Charifson, P. S.; Bowen, J. P.; Wyrick, S. D.; Hoffman, A. J.; Cory, M.; McPhail, A. T.; Mailman, R. B. *J. Med. Chem.* **1989**, *32*, 2050.
19. Heightman, T. D.; Wilson, D. M. U.S.A. Patent WO/2004/035544 *Free Patents online* **2004**, 33.
20. Spinks, D.; Armer, R. E.; Miller, D. J.; Rankovic, Z.; Spinks, G.; Mestres, J.; Jaap, D. R. U.S.A. Patent, *Free patents online* **2003**, 41.
21. Molinari, A. J.; Ashwell, M. A.; Ridgway, B. H.; Failli, A. A.; Moore, W. J. U.S.A. Patent 2004/050631, *Free Patents online* **2004**, 203.
22. Yamamoto, H.; Pandey, G.; Asai, Y.; Nakano, M.; Kinoshita, A.; Namba, K.; Imagawa, H.; Nishizawa, M. *Org. Lett.* **2007**, *9*, 4029.
23. Fisher, G. H.; Moreno, H. R.; Oatis, J. E.; Schultz, H. P. *J. Med. Chem.* **1975**, *18*, 746.
24. Nieto, M. J.; Alovero, F.; Manzo, R. H.; Mazzieri, M. R. *Eur. J. Med. Chem.* **1999**, *34*, 209.
25. *Exploring QSAR*; Hansch, C., Leo, A., Eds. Fundamentals and Application in Chemistry and Biology; ACS Publications, 1995.
26. Atsuko, N.; Tadahi, K. *Chem. Pharm. Bull.* **1984**, *32*, 2421.
27. Togo, H.; Hoshina, Y.; Muraki, T.; Nakayama, H.; Yokoyama, M. *J. Org. Chem.* **1998**, *63*, 5193.
28. Togo, H.; Hoshina, Y.; Yokoyama, M. *Tetrahedron Lett.* **1996**, *37*, 6129.
29. Kneisel, F. F.; Monguchi, Y.; Knapp, K. M.; Zipse, H.; Knochel, P. *Tetrahedron Lett.* **2002**, *43*, 4875.
30. Kubo, T.; Katoh, C.; Yamada, K.; Okano, K.; Tokuyama, H.; Fukuyama, T. *Tetrahedron* **2008**, *64*, 11230.
31. Frisch, M. J.; G. W. T., Schlegel, H. B.; Scuseria, G. E.; Robb, J. R. Cheeseman, M. A.; Montgomery, Jr., J. A.; Vreven, T.; Kudin, K. N.; Burant, J. C.; Millam, J. M.; Iyengar, S. S.; Tomasi, J.; Barone, V.; Mennucci, B.; Cossi, M.; Scalmani, G.; Rega, N.; Petersson, G. A.; Nakatsuji, H.; Hada, M.; Ehara, M.; Toyota, K.; Fukuda, R.; Hasegawa, J.; Ishida, M.; Nakajima, T.; Honda, Y.; Kitao, O.; Nakai, H.; Klene, M.; Li, X.; Knox, J. E.; Hratchian, H. P.; Cross, J. B.; Bakken, V.; Adamo, C.; Jaramillo, J.; Gomperts, R.; Stratmann, R. E.; Yazyev, O.; Austin, A. J.; Cammi, R.; Pomelli, C.; Ochterski, J. W.; Ayala, P. Y.; Morokuma, K.; Voth, G. A.; Salvador, P.; Dannenberg, J. J.; Zakrzewski, V. G.; Dapprich, S.; Daniels, A. D.; Strain, M. C.; Farkas, O.; Malick, D. K.; Rabuck, A. D.; Raghavachari, K.; Foresman, J. B.; Ortiz, J. V.; Cui, Q.; Baboul, A. G.; Clifford, S.; Cioslowski, J.; Stefanov, B. B.; Liu, G.; Liashenko, A.; Piskorz, P.; Komaromi, I.; Martin, R. L.; Fox, D. J.; Keith, T.; Al-Laham, M. A.; Peng, C. Y.; Nanayakkara, A.; Challacombe, M.; Gill, P. M. W.; Johnson, B.; Chen, W.; Wong, M. W.; Gonzalez, C.; Pople, J. A. Gaussian, Inc: Wallingford CT, 2004.
32. Katritzky, A. R.; Akhmedov, N. G.; Myshakin, E. M.; Verma, A. K.; Dennis Hall, C. *Magn. Reson. Chem.* **2005**, *43*, 351.
33. Chilmonczyk, Z.; Cybulski, J.; Szelejewska-Wozniakowska, A.; Leg, A. J. *Mol. Struct.* **1996**, *385*, 195.
34. Amm, M.; Palatzer, N.; Bouchet, J. P.; Volland, J. P. *Magn. Reson. Chem.* **2001**, *39*, 77.
35. Sanchez-Viesca, F.; Berros, M.; Gómez, M. R. *Heterocycl. Commun.* **2003**, *9*, 5.
36. Sanchez-Viesca, F.; Berros, M. T. I. P. *Rev. Especializada Cien. Quim.-Biol.* **2006**, *9*, 10.
37. Sanchez-Viesca, F.; Nicolás, I.; Berros, M. T. I. P. *Rev. Especializada Cien. Quim.-Biol.* **2004**, *7*, 5.
38. Desiraju, G. R. *Acc. Chem. Res.* **1991**, *24*, 6.
39. *The Weak Hydrogen Bond in Structural Chemistry and Biology*; Desiraju, G. R., Steiner, T., Eds.; Oxford University press, 1999.
40. Taylor, R.; Kennard, O. *J. Am. Chem. Soc.* **1982**, *104*, 7.
41. De Benedetti, P. G.; Iarossi, D.; Folli, U.; Frassinetti, C.; Menziani, M. C.; Cennamo, C. *J. Med. Chem.* **1989**, *32*, 2396.
42. De Benedetti, P. G. *Prog. Drug Res.* **1991**, *36*, 361.
43. Jorgensen, W. L. *Science* **2004**, *303*, 1813.
44. Ganapaty, S.; Steve Thomas, P.; Karagianis, G.; Waterman, P. G.; Brun, R. *Phytochemistry* **2006**, *67*, 1950.